

Photoluminescence properties of Tb_2O_3 embedded in the TiO_2 nanocrystals

Haeyoung Choi^a, Jung Hwan Kim^{a,*}, Soung-soo Yi^b, Byung Kee Moon^c,
Jung Hyun Jeong^c

^a Department of Physics, Donggeui University, Busan 614-714, Republic of Korea

^b Department of Photonics, Silla University, Busan 617-736, Republic of Korea

^c Department of Physics, Pukyong National University, Busan 609-737, Republic of Korea

Received 31 July 2004; received in revised form 16 December 2004; accepted 13 January 2005

Available online 24 June 2005

Abstract

Nanosize terbium oxide embedded in the TiO_2 nanocrystal has been produced using a reverse micellar synthesis. High-resolution transmission electron microscopy and X-ray diffraction measurements have identified particles with a size of 4.5–5.5 nm in the anatase phase. The time resolved spectroscopic technique has been used for the measurement of luminescence spectra and decay curves. Strong emissions from 5D_4 levels of Tb^{3+} ions were detected at the sample having core (Tb_2O_3)–shell (TiO_2) structure. The structure of this luminescence spectrum was anomalous which has very strong emission band due to the transition of $^5D_4 \rightarrow ^7F_2$. It was ascribed to two kinds of energy migration among Tb^{3+} ions ($^5D_4 \rightarrow ^7F_6$ and $^5D_4 \rightarrow ^7F_2$) in terbium oxide nanoparticle and quenching centers located at the boundary between core and shell. The excitation energy corresponding to the transition of $^5D_4 \rightarrow ^7F_2$ may be able to migrate among Tb^{3+} ions for a long time, since the quenching centers operate upon higher excitation energy than that of this migration.

© 2005 Elsevier B.V. All rights reserved.

Keywords: Nanocrystals; Titania; Terbium; Photoluminescence

1. Introduction

TiO_2 has attracted much attention in many years because of its applications and physical properties, which show interesting variations influenced by oxygen defects, impurities and crystalline modifications. The photocatalytic activity of titania is greatly influenced by its crystal structure, particle size, surface area and porosity [1]. There have been few reports on rare earth doped semiconductor nanoparticles as it is difficult to incorporate rare earth ions effectively in nanocrystals. Luminescent nanoparticles have attracted increasing technological and industrial interest. This interest has mainly to do with their optical properties that affect emission lifetime, structure of emission spectra, luminescence quantum efficiency and concentration quenching. Recently, optical spec-

troscopy of rare earth doped nano-oxides has been studied by many investigators [2–4] in order to improve for advanced phosphor and photonic materials. It has been shown that the successful synthesis of lanthanide oxides nanoparticles can be achieved by a number of process, including sol–gel methods [5], hydrothermal technique [6] and the reverse micelle method [7,8]. Reverse micelles represent an interesting controlled water environment in which to study luminescent properties of lanthanides.

However, luminescence of terbium doped in titania nanoparticle has not been reported as far as we know. In this paper, we try to get luminescence that is emitted from terbium embedded in the titania nanocrystals. We prepared nanoparticles having core (Tb_2O_3)–shell (Ti_2O_3) structure using a reverse micellar synthesis that was developed by Li et al. [8]. The products were examined by X-ray diffraction, transmission electron microscopy for characterizing their structure and particle size distribution. From measuring

* Corresponding author. Fax: +82 51 890 1490.
E-mail address: kimjh@deu.ac.kr (J.H. Kim).

the luminescence spectra and lifetimes by the time-resolved spectroscopic technique, we discuss some possible energy transfer processes. And we propose a model for the mechanism of anomalous Tb^{3+} luminescence in the core-shell nanoparticles.

2. Experimental

Terbium nitrate pentahydrate ($\text{Tb}(\text{NO}_3)_3 \cdot 5\text{H}_2\text{O}$) was dissolved in 0.27 g water and mixed with 30 g anhydrous toluene ($\text{C}_6\text{H}_5\text{CH}_3$, 99.8%, Aldrich) and 1.413 g oleic acid. Then, 1.706 g titanium isopropoxide (TIP, $\text{Ti}(\text{OHC}(\text{CH}_3)_2)_4$, 97%, Aldrich) dissolved in anhydrous 5 g toluene was added. All reagents were used without any further purification process and mixed in a glove box with argon atmosphere. Different concentrations of terbium nitrate pentahydrate (2.0, 5.0 and 10.0 mol%) were dissolved in solvent. The mixture was vigorously stirred with a magnetic stirrer for 24 h and transferred into a stainless-steel autoclave with a teflon liner (80 ml capacity, 60% filling). And then it was heated to 250 °C to remove the organic materials with a rate of 4 °C/min and maintained for 20 h without stirring. After cooling gradually to room temperature, the mixture was separated with centrifugal separator and then dried in vacuum. The nanocomposites were sintered at 500 °C for 3 h.

The collected nanophosphor particles were characterized by X-ray diffraction (X'Pert-MPD System, PHILIPS) and transmission electron microscopy (TEM, JEM-2010 JEOL, H-7500, HITACHI). Average particle size of nanocrystalline TiO_2 was calculated from the width of the XRD peaks of (1 0 1) plane using the Scherrer equation [9,10] and also measured by the image analysis of transmitted electron micrograph (TEM). The composition ratio of nanoparticles was analyzed by energy dispersive X-ray spectrometer (EDS). We measured the luminescence spectra and lifetimes by the time-resolved spectroscopic technique. The excitation source was a Q-switching Nd:YAG laser with pulse duration of 5 ns and a repetition rate of 10 Hz. The excitation wavelength was 355 nm in order to pump not terbium oxide but titania. The emitted light was focused into a 75-cm monochromator and detected by a thermoelectrically cooled photomultiplier tube. The signal was fed to a photon-counting system (DM 3000, SPEX) or to a digital oscilloscope (LeCroy 9450 A).

3. Results and discussion

The TEM micrograph of the nanoparticles is shown in Fig. 1. Nanoparticles have polyhedral-shaped morphologies and good electron diffraction patterns, which indicates that they have crystalline nature with good crystallinity. The TEM measurements have shown that the average size of particles was similar to each others as 4.5–5.5 nm although the amount of Tb content is different.

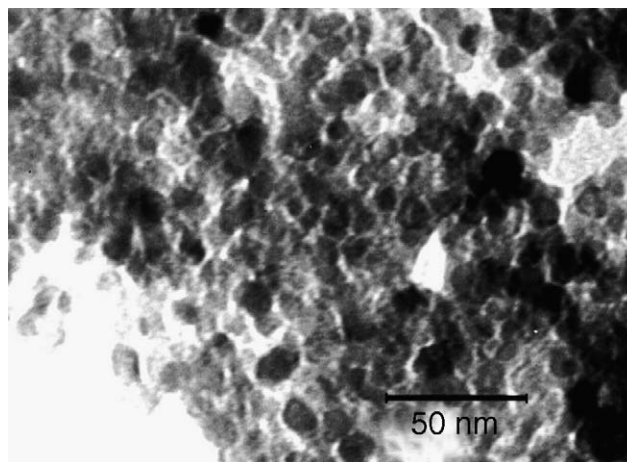


Fig. 1. TEM photograph of nanoparticles having core (Tb_2O_3)–shell (TiO_2) structure prepared by reverse micellar method.

Exciting the titania in its band gap results in energy transfer to the emitting state of rare earth ions, luminescence of some kind of rare earth ions takes place. But, luminescence of terbium doped in titania has not been reported as far as we know. Frindell et al. [11] reported that luminescence of terbium in titania was not observed, since the energy levels of the emitting state of Tb^{3+} ion are higher than that of the trap states of titania. These states that may be operated as quenching centers are created by introducing terbium ions in the titania and the kinds of quenching centers have not known yet. It has been reported by different authors [11–13] that the energy levels of the trap states in the titania nanocrystallites are located between 2.35 and 2.59 eV (475–525 nm).

Fig. 2 shows luminescence spectra of the sample at 13 K, which contains 5 mol% terbium and was heated at 650 °C for 10 h. It may be considered that the core-shell structure was changed into homogeneous doping structure by thermal diffusion of the ions. As can be seen in Fig. 2(a), there are three kinds of excitons peaks and no emission of the Tb^{3+} ions. It was found that the lifetimes of the three broad peaks were 1.1 ns (435 nm), 290 μs (535 nm) and 300 μs (650 nm),

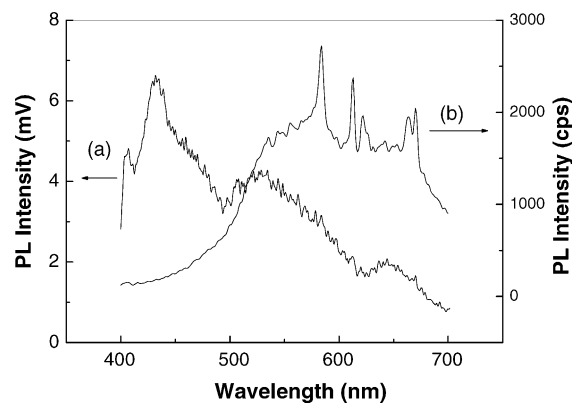


Fig. 2. Luminescence spectra of dispersed Tb^{3+} ions in titania nanoparticles using direct current mode (a) and photon-counting system (b).

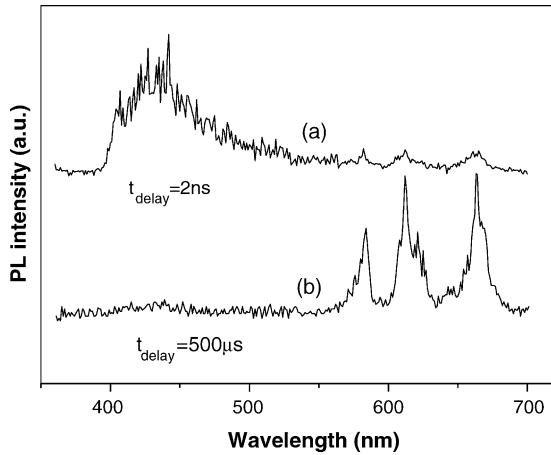


Fig. 3. Time resolved luminescence spectra of nanoparticles having core (Tb_2O_3)–shell (TiO_2) structure.

respectively. Since the resolution of our time resolved spectroscopic system was 5 ns, the lifetime of broad emission centered at 435 nm was assumed to be sub-nano second. It was reported that the broad band centered at 435 nm is due to the free excitons of the titania nanoparticles [13,14], and the broad emission bands at 535 and 650 nm are attributed to oxygen vacancy levels [12]. Since the emissions radiated by the recombination of free excitons disappear within several nanoseconds, these signals cannot be detected by photon-counting system (PC mode). Therefore, strong broad emission centered at 435 nm is disappeared in the spectrum (b) that was obtained by PC mode. On the other side three weak emission bands from Tb^{3+} ions can be seen in this spectrum at 580 nm ($^5\text{D}_4 \rightarrow ^7\text{F}_4$), 617 nm ($^5\text{D}_4 \rightarrow ^7\text{F}_3$) and 664 nm ($^5\text{D}_4 \rightarrow ^7\text{F}_2$). Unusually, no emissions in the green ($^5\text{D}_4 \rightarrow ^7\text{F}_5$), blue ($^5\text{D}_4 \rightarrow ^7\text{F}_6$) and ultraviolet spectral region from the higher energy $^5\text{D}_3$ level are observed.

Fig. 3 shows the time resolved spectra of the nanoparticles by using direct current mode (DC mode) at room temperature. The nanoparticles having core–shell structure were prepared by reverse micelles methods and were sintered at 500 °C for 3 h in order to remove organic materials. As shown in Fig. 3, in the short delay time, only a broad free exciton band appears at 435 nm, and two bands that are shown in Fig. 2(a) disappear. Emission due to the excitations at room temperature, which is impossible for bulk titania, was found for nanostructured titania and this phenomenon was thought to result from spatial confinement and dielectric confinement. Considering disappeared two emission bands are attributed to oxygen vacancy levels that are promoted by introducing of terbium in the titania [12], it is believed that the nanoparticle sintered at 500 °C preserves core–shell structure. In the long delay time of 500 μs, three strong bands emitted from Tb^{3+} ions are shown in Fig. 3(b). Since lifetimes of Tb^{3+} ions are much longer than that of excitons, the color of the sample was seen as orange with the naked eye at room temperature. And the color of the sample was gradually changed to bright white with decreasing temperature, because the emission intensity

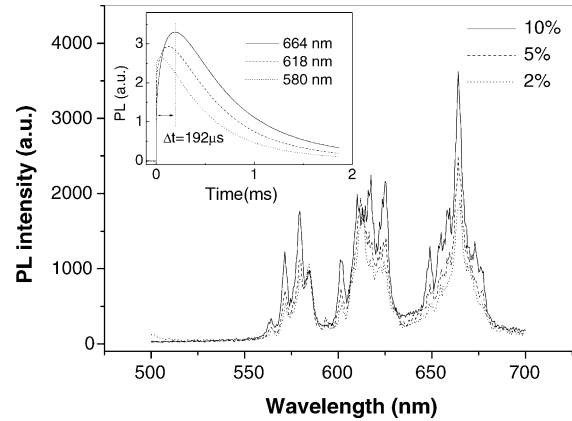


Fig. 4. Luminescence spectra of nanoparticles having core (Tb_2O_3)–shell (TiO_2) structure. Inset: decay curves of emission from $^5\text{D}_4:\text{Tb}^{3+}$ ions to $^7\text{F}_4$ (580 nm), $^7\text{F}_3$ (618 nm) and $^7\text{F}_2$ (664 nm), respectively.

of the free exciton band was increased with decreasing of temperature.

Fig. 4 exhibits the luminescence spectra of Tb^{3+} ions emitted from the core (Tb_2O_3)–shell (TiO_2) nanoparticles with the different concentration of terbium at room temperature, where 2, 5 and 10% denote the average ratios of the numbers of atoms (Tb/Ti). It is worth noting that concentration quenching of terbium in nanoparticles is very weak comparing to that in the bulk, which is characteristic of nanoparticles. The luminescence spectra of Tb^{3+} ions as can be seen in Fig. 4 were very different from that of Tb_2O_3 nanoparticles [15] and of $\text{Gd}_2\text{O}_3:\text{Tb}^{3+}$ nanoparticles [16]. The luminescence spectra in these references are very similar and energy level diagram of Tb^{3+} ion can be seen in reference [15]. Three emission bands from $^5\text{D}_4$ level to $^7\text{F}_J$ levels of Tb^{3+} ions can be seen in these spectra at 580 nm ($J=4$), 617 nm ($J=3$) and 664 nm ($J=2$). Actually, terbium ions have been used for green phosphors because $J=5$ branching ratio is much higher than the others, however, there are no emission bands from the transitions to $J=6$ (blue) and $J=5$ (green) levels in these spectra. The relative emission intensities from $^5\text{D}_4$ level to different J levels were 19% ($J=4$), 38% ($J=5$) and 43% ($J=2$), respectively. In order to assign the anomalous emission spectrum of Tb^{3+} in our sample, we proposed two kinds of energy migration among Tb^{3+} ions ($^5\text{D}_4 \rightarrow ^7\text{F}_6$ and $^5\text{D}_4 \rightarrow ^7\text{F}_2$) in core nanoparticles, and quenching centers located at the interface between core (Tb_2O_3) and shell (TiO_2). Considering no emission bands of blue and green, the quenching centers powerfully operate upon higher excitation energy. Under 355 nm excitation, exciting the titania in its band gap results in energy transfer to the level $^5\text{D}_{3,4}$ of terbium oxide embedded in titania. Then, $^5\text{D}_4$ levels are more populated by cross-relaxation of Tb^{3+} in core. The cross-relaxation ($^5\text{D}_3 + ^7\text{F}_{1,2} \rightarrow ^5\text{D}_4 + ^7\text{F}_6$) may be a phonon assisted process, where final states are $^7\text{F}_2$ and $^5\text{D}_4$ states. Usually in the TiO_2 nanoparticles, the migration of $^5\text{D}_4 \rightarrow ^7\text{F}_6$ can be possible in the early stage, because the $^7\text{F}_6$ level is ground states. According to the inset of Fig. 4, the rise

time of 580 nm emission radiated by the $^5D_4 \rightarrow ^7F_4$ transition was shorter than 10 μ s. However, the rise time of 664 nm emission radiated by $^5D_4 \rightarrow ^7F_2$ transition was delayed by 192 μ s. It is ascribed the 7F_2 states are populated by the cross-relaxation and another migration of $^5D_4 \rightarrow ^7F_2$ can be followed by cross-relaxation. In short, the luminescence in our sample is emitted while energy migrations occur in terbium oxide before passing to quenching centers. Since the quenching centers powerfully operate upon the higher excitation energy, instantaneous migration of $^5D_4 \rightarrow ^7F_6$ reaching to the center result in no emission of blue and green. But the excitation energy corresponding to the transition for $^5D_4 \rightarrow ^7F_2$ may be able to migrate among Tb_{3+} ions for a long time, and thus this transition gets many opportunities to emit light.

4. Conclusion

Nanosize terbium oxides embedded in the TiO_2 nanocrystal have been produced using a reverse micellar synthesis. High-resolution transmission electron microscopy and X-ray diffraction measurements have identified particles with a size of 4.5–5.5 nm in the anatase phase. During 650 °C, annealing of the sample having core–shell structure for 10 h, it may be considered that core–shell structure changed into homogeneous doping structure by thermal diffusion of the ions. In this sample, very weak emission radiated from Tb^{3+} ions have been found. However, strong emissions from $^5D_4:Tb^{3+}$ were found in the sample sintered at 500 °C. This sample may be preserved core (Tb_2O_3)–shell (TiO_2) structure. The color of this emission was seen as orange by naked eyes at room temperature, although Tb^{3+} ions are used for green phosphors. Especially, the emission band centered at 664 nm due to the transition from 5D_4 to 7F_2 level was very strong. This phenomenon can be explained as follows. The luminescence of the $^5D_4:Tb^{3+}$ is emitted while energy migrations occur in terbium oxide before reaching to quenching center due to the interface between core and shell. The excitation

energy corresponding to the transition of $^5D_4 \rightarrow ^7F_2$ may be able to migrate among Tb^{3+} ions for a long time and thus this transition gets many opportunities to emit light, since the quenching centers operate upon higher excitation energy than that of this migration.

Acknowledgement

This work was supported by Korea Research Foundation Grant (KRF-2003-037-C00020).

References

- [1] U. Diebold, Surf. Sci. Rep. 48 (2003) 53.
- [2] B.M. Tissue, Chem. Mater. 10 (1998) 2837.
- [3] M. Hasse, K. Riwoński, H. Meyssana, A. Kornowski, J. Alloys Compd. 303–304 (2000) 191.
- [4] A. Huignard, T. Gacoin, J.P. Boilot, Chem. Mater. 12 (4) (2000) 1090.
- [5] M. Morita, D. Rau, H. Fujii, Y. Minami, S. Murakami, M. Baba, M. Yoshita, H. Akiyama, J. Lumin. 87–89 (2000) 478.
- [6] Y. Hakuta, Y. Haganuma, K. Sue, T. Adschiri, K. Arai, Mater. Res. Bull. 38 (2003) 1257.
- [7] S.D. Romano, D.H. Kurlat, Chem. Phys. Lett. 323 (2000) 93.
- [8] T. Li, J. Moon, A. Morrone, J. Mecholsky, D. Talham, J. Adair, Langmuir 15 (1999) 4328.
- [9] K.M. Reddy, C.V.G. Reddy, S.V. Manorama, J. Solid State Chem. 158 (2001) 180.
- [10] B.D. Cullity, Elements of X-Ray Diffraction, second ed., Addison–Wesley, Reading, MA, 1978.
- [11] K.L. Frindell, M.H. Bartl, M.R. Robinson, G.C. Basen, A. Popitsch, S. Stucky, J. Solid State Chem. 172 (2003) 81.
- [12] P.M. Kumar, S. Badrinarayanan, M. Sastry, Thin Solid Films 358 (2000) 122.
- [13] Y.C. Zhu, C.X. Ding, J. Solid State Chem. 145 (1999) 711.
- [14] Y. Zhu, C. Ding, G. Ma, Z. Du, J. Solid State Chem. 139 (1998) 124.
- [15] G. Wakefield, H.A. Keron, P.J. Dobson, J.L. Hutchison, J. Phys. Chem. Solids 60 (1999) 503.
- [16] R. Bazzi, M. Flores-Gonzalez, C. Louis, K. Lebbou, C. Dujardin, A. Brenier, W. Zhang, O. Tillement, E. Bernstein, P. Perriat, J. Lumin. 102–103 (2003) 445.